Design and development of laser Doppler velocimetry based on DSP technique for blood flow measurement

Yuan-Hsiang Lin, Yan-Yu Chen, Yuan Ho, Yi-Lin Li, and Gwo-Jen Jan*
Department of Electrical Engineering, National Taiwan University

ABSTRACT

A graphic user interface and real-time laser Doppler velocimeter (LDV) based on the digital signal processor (DSP) had been designed and developed. The hardware setup included the Michelson interferrometer optics, photo-detector, current to voltage converter, AC amplifier and filtering circuits, as well as a DSP module. The software system on DSP module was also developed to access data and to perform the moment weighting algorithms. In addition, the processed data was transmitted to the personal computer and advanced analysis could be achieved. The velocity measurement using developed LDV device was calibrated by a mirror mounted on a linear vibrator. The outcomes presented high linearity and good accuracy. In vitro experiment employing this LDV system was also carried out. The results showed that the developed LDV instrument offered a flexible tool to investigate the blood flow of microcirculation system.

Keywords: Laser Doppler, Blood flow, Digital Signal Processor (DSP)

1. INTRODUCTION

In recent years, scientists have devoted to investigating how the circulation diseases influence microvascular flow[1]. Some relations were found and early-stage detection of these diseases can be achieved by continuous monitoring of microcirculation. Among various measuring techniques, laser Doppler velocimetry (LDV) has been adopted most widely. Since first introduced by M.D. Stern[2] in 1975, LDV is now well established and extensively used in skin perfusion measurements. Other applications to monitor choroidal flow[3], renal arterioles[4] and microcirculation in gums were also developed. Because the technique is non-invasive and highly spatial sensitive, so far it can hardly be replaced by any other methods in physiology measurement.

However, though LDV provides such advantages, there are still some problems to be solved[5]. Since the scattering mechanism is too complicated to be determined in tissue[6], various algorithms[7,8] are developed to obtain indicators for fluid velocity. Applying different algorithms, the results may somewhat differ. In addition, the processing bandwidth[9] is also involved. Adopting low cut-off frequency may lead to under-estimation of velocity while using high cut-off frequency limits the frequency resolution. Besides, the computed result is closely related to the penetration depth[10], which is decided by the laser used[11]. With different penetration depths, different volumes are sampled; and it's hard to say which interprets the fluid velocity better. More than that, absolute in vivo calibrations of LDV systems are difficult to achieve due to the large variation in cutaneous structure[12].

Therefore, in this study we developed a digital signal processor (DSP) based LDV system and a simplified physical model was also implemented for the in vitro experiment. By applying the DSP framework, we evaluated the linearity of different algorithms, and determined a linear indicator for the fluid velocity.

In *Optical Sensing, Imaging, and Manipulation for Biological and Biomedical Applications*, Robert R. Alfano, Ping-Pei Ho, Arthur E. T. Chiou, Editors, Proceedings of SPIE Vol. 4082 (2000) • 0277-786X/00/$15.00

2. THEORY AND COMPUTATION ALGORITHMS

When a photon is scattered by a moving particle, the light frequency is slightly shifted. The Doppler frequency-shift $\triangle f$ is given by[13]

$$\triangle f = (|\mathbf{k}||\mathbf{v}|/\pi)\sin^{1}/_{2}\theta\cos\alpha \tag{1}$$

where **k** is the incoming wave vector ($\mathbf{k} = 2\pi/\lambda$, λ is the wavelength), **v** is the velocity of the moving particle, θ is the scattering angle, and α is the angle between $\triangle\mathbf{k}$ and **v**.

Applying Doppler effect on skin perfusion measurement, the situation becomes much more difficult due to the complicated scattering mechanism in tissue. The intensity modulation of the detected signal shows an approximately exponential decay in the spectra. Bonner and Nossal's[14] results showed that the first (weighted) moment $\langle\omega\rangle$ of the spectral power density $S(\omega)$ of the detector signal is linearly proportional to the average velocity $\langle v\rangle$ of all moving particles in the optical sampling volume. The first weighted moment (FWM) is expressed as

$$\langle v\rangle \sim \langle\omega\rangle = M_1 / M_0, \text{ with } Mn \equiv \int_{-\infty}^{\infty}\omega^n S(\omega)d\omega. \tag{2}$$

The numerator M_1 is the first moment of the spectral power density $S(\omega)$. It is assumed to be proportional to the blood flow rate in the optical sampling volume. The denominator M_0 is proportional to the total amount of Doppler-shifted light.

The second weighted moment (SWM) is expressed as

$$\langle v^2\rangle \sim \langle\omega^2\rangle = M_2 / M_0 = \frac{\int_{-\infty}^{\infty}\omega^2 S(\omega)d\omega}{\int_{-\infty}^{\infty}S(\omega)d\omega}. \tag{3}$$

Square root of $\langle v^2\rangle$ represents the RMS value of blood velocity, and can be regarded as another representative of the blood velocity.

After the calculation of the first and second weighted moments, the results can be derived, in the unit of frequency (Hz) instead of velocity (m/s). The calculated value is proportional to the blood velocity, and a conversion factor should be added to compute the fluid velocity. However, the conversion factor varies between individuals and even between different sites on an individual. Thus we adopted an linear indicator to represent the fluid velocity instead of the absolute value.

3. INSTRUMENTATION

3.1. Hardware Setup

The block diagram of the LDV hardware system is shown in Fig. 1. It includes an optical system, analog signal conditioning circuits, a DSP module and a graphic user interface (GUI). The optical system contains a 5mW laser diode (650nm) and/or He-Ne laser (632.8nm), a test object, and an optical detector. It detects the optical heterodyne and converts the signal into electrical domain. In analog module, the preamplifier initially amplifies the weak signal and transforms photocurrent to voltage (gain is 200 V/mA). The AC amplifier further amplifies the AC signal and the gain is depending on the light intensity (max. gain is 200). The total bandwidth of the analog module is 50kHz.

The DSP module consists of a 16 bit, 200 kHz sampling rate ADC for A/D conversion, a 32k-byte EEPROM for program storage, high speed SRAMs up to 128k-word for DSP data buffer, and a TMS320C31 DSP as well as an ADS7843 touch-screen controller. In this module, a 2048-points Fast Fourier Transform (FFT) is performed on DSP. The sampling

rate is 200kHz and the frequency resolution is 97.7Hz. According to equation (1), in simulation experiment (λ=632.8nm) the maximal measurable velocity is 15.82mm/s and velocity resolution is 30.9μm/s in this system that are depended on θ and α. The GUI consists of a 240×128 dots graphic LCD and a touch screen panel. The touch screen allows a user to enter a command simply by touching a location on the panel. The two devices together make the user interface more friendly and easy to use. In the other hand, the DSP can transfer the results to PC in real-time through RS-232 interface, and data analysis and storage can be further achieved. It has flexibility to modify the computing algorithm of velocity of DSP through the control panel of PC.

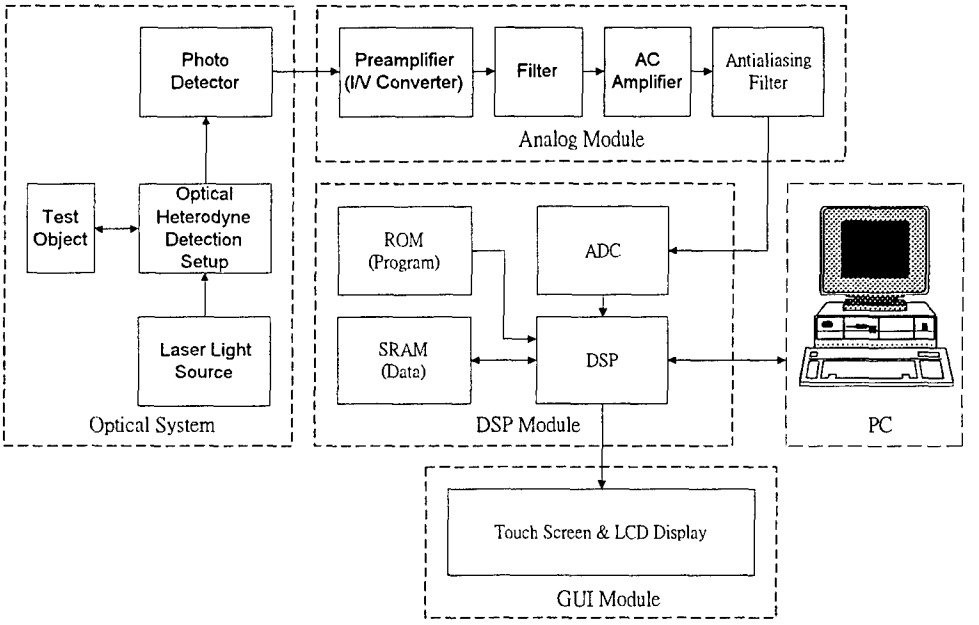

Fig. 1 The block diagram of the LDV hardware system

3.2. Software Development

The main flowchart of our program is shown in Fig. 2. After power on, program starts at initializing all control registers of DSP and LCD. Then program goes into the major loop, which makes the DSP wait for sample data to fill an input buffer, perform FFT on the data to obtain the power spectrum, calculate blood velocity based on the spectrum, then display it and carry out any user input. For the requirement of real-time processing, all source codes were written in C3x assembly language instead of other high-level languages.

The FFT used in the program is a 2048-point, decimation in time algorithm. Powered by the bit-reverse addressing mode and parallel instructions of the C3x DSP, the FFT can be calculated in a very short period of time. With a sampling rate of 200kHz, the frequency resolution df is

$$df = \frac{200k}{2048} = 97.7Hz\,. \tag{4}$$

Sampling of signal goes continuously, and every 5μsec DSP will receive a new sample data from ADC. To prevent new data from mixing with data that are currently under processing, a three buffer rotating technique is used. Input buffer accumulates new data coming from ADC. The data in FFT buffer are those currently under processing (FFT or calculation of blood velocity), and output buffer stores previously processed data, which is used for the spectrum display.

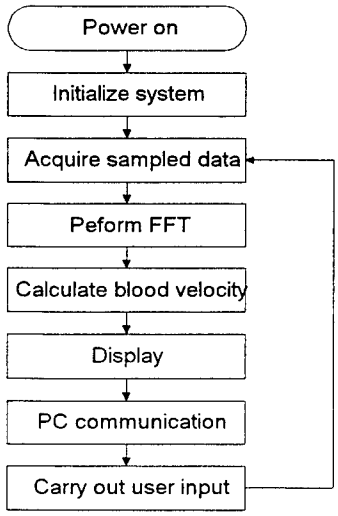

Fig. 2 The flowchart of the main program

When sample data fills the input buffer, a buffer rotating occurs. The input buffer becomes FFT buffer so that its contents are ready for FFT calculation. FFT buffer becomes output buffer and the spectrum stored in it will be displayed immediately. Output buffer becomes input buffer and will start accepting new sample data.

The calculation of blood velocity involves three algorithms –FWM, SWM, and the peak value of the frequency (PVF) methods. PVF was devised by us and is simply the selection of the frequency that has maximum power in the power spectrum. Since the power spectrum stored in memory is actually in discrete form, the integration of equation (2) must be approximated by the following summation:

$$FWM = \frac{\sum_{n=n1}^{n2} ndf \cdot S[n]}{\sum_{n=n1}^{n2} S[n]}. \tag{5}$$

Where df is the same as in equation (4) and S[n] is the power spectrum after FFT calculation. It is obvious that frequencies lower than $n1 \cdot df$ and those higher than $n2 \cdot df$ will be excluded from the calculation of blood velocity. Thus by choosing the value of $n1$ and $n2$, a thresholding mechanism is easily implemented, with $n1 \cdot df$ and $n2 \cdot df$ being the lower and upper threshold. Proper use of this thresholding mechanism can eliminate unwanted frequency components like high frequency noises or the large DC component in the signal spectrum.

Similarly the calculation of SWM uses the following summation form instead of the integration form in equation (3).

$$SWM = Sqrt\left(\frac{\sum_{n=n1}^{n2}(ndf)^2 \cdot S[n]}{\sum_{n=n1}^{n2} S[n]}\right) \tag{6}$$

The PVF algorithm was implemented using a simple compare-and-update algorithm for finding the frequency that has largest power in the signal spectrum.

4. EXPERIMENTS

4.1. Simulation Experiment

FWM, SWM, and PVF methods are designed to calculate the velocity of a moving object. The simulation experiment is to check the computation of the algorithms and to calibrate the LDV device. The experimental setup is shown in Fig. 3. A 632.8nm He-Ne laser provides a light beam which pass through the beam splitter (50:50) and splits into two. One beam hits the moving mirror and is Doppler frequency shifted. The other hits a stationary mirror and keeps its frequency non-shifted. The reflected beams are collected by an optical fiber and picked up by a detector.

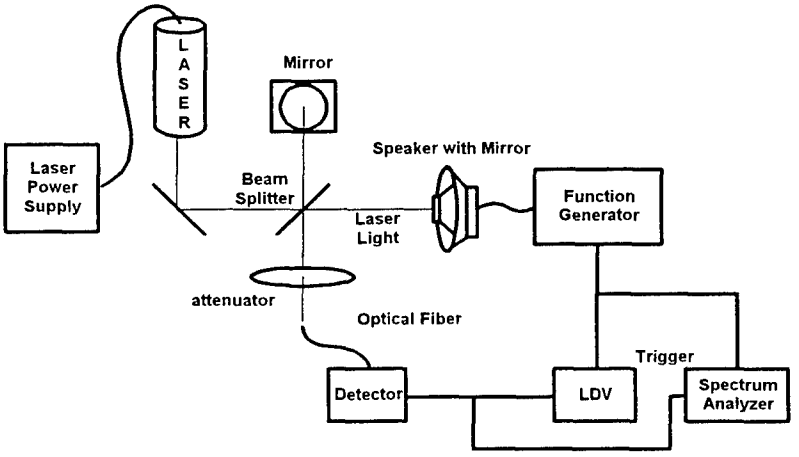

Fig. 3 The block diagram of measurement system setup for simulation experiment

The moving mirror is mounted on the front surface of a speaker center. A function generator outputs a triangular wave to the speaker and vibrates the mirror. In the forward and backward motion of the speaker, the mirror on its center would have a constant velocity. The relationship between applied voltage and speaker displacement has be measured. The linear relationship from the experiment measurement is shown in Fig. 4.

For the forward motion, the speaker kept pushing the mirror forward in velocity v, which can be calculated from frequency and peak-to-peak voltage of the triangular wave. For convenience the backward motion is neglected. The trigger signal from the function generator is connected to the LDV, which could be set to trigger mode so that it functioned only for the forward motion of the speaker, be sure the measured velocity is constant. If the shifted frequency hasn't be triggered, the

peak would vibration in the spectrum. This function also could be used to investigate the sequence relation of ECG signal and the blood flow in microcirculation.

Applying Doppler frequency shift equation (1) we get

$$\Delta f(kHz) = 3.161 \times v(mm/s) \tag{7}$$

where Δf is Doppler frequency shift, v is Mirror velocity.

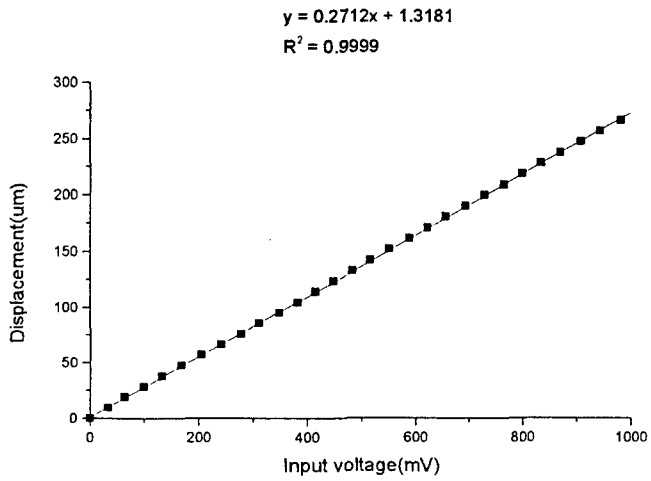

Fig. 4 Displacement calibration curve of a vibrating mirror

Note that this conversion factor between frequency and velocity is valid only in this simulation, and cannot be applied to any other situations. By changing the peak-to-peak voltage of the triangular wave, the velocity of the mirror changed as well. For each velocity the outputs of the three algorithms (FWM, SWM, and PVF) were recorded. The results are discussed in the following section.

4.2.In Vitro Experiment

In order to evaluate our system, we developed a simplified close-loop model, in which the linearity of various algorithms can be tested. The schematic diagram of the setup is shown in Fig. 5. In this model, micro-spheres were added into the water to serve as scattering particles (mass concentration = 0.1 %), and a DC motor with a precise controller was also employed to pump the solution. The photo-detector of the LDV picked up the light signals scattered either by the moving particles or the static tube. The Doppler shifted and non-shifted parts of the scattered beams heterodyned at the photodiode and produced corresponding photocurrent. After being amplified, the analog signals were translated into digital signals and a FFT processing was performed. Deriving this information in the frequency domain, we applied different algorithms to search for a linear transformation between the frequency spectrum and the fluid velocity. The processed data were transmitted to the PC, and advanced analysis could be taken.

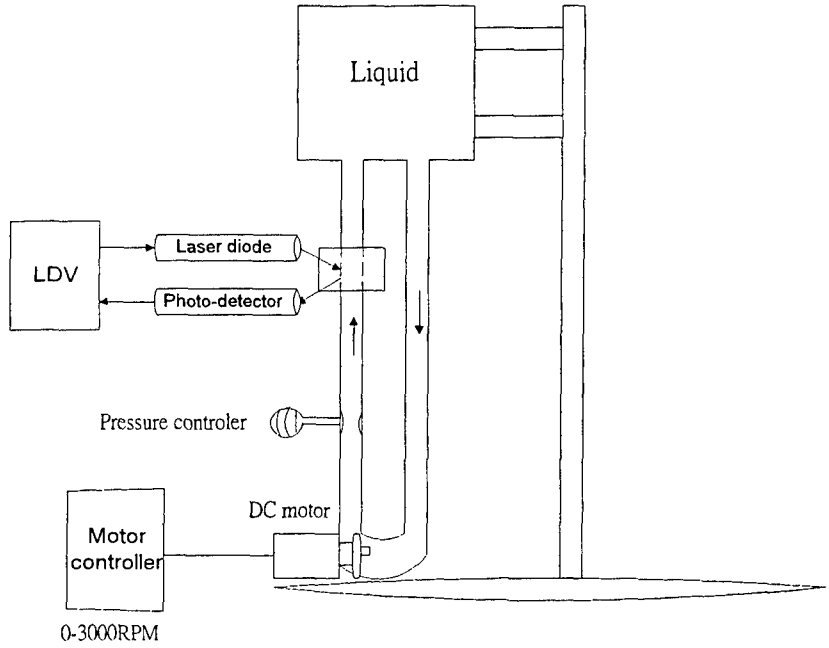

Fig. 5 Experimental setup for in vitro measurement

5. RESULTS AND DISCUSSION

5.1. Simulation Experiment

The design value of the mirror velocity can be calculated from the displacement measurement and vibrating period. The measured values using the FWM, SWM algorithms and PVF method are originally in terms of frequency unit (Hz) and are converted to the unit of velocity (mm/s) using equation (7). The comparison between designed value and measured value was displayed in Fig. 6 (A), (B), and (C). As the figure shows, all three algorithms gave values lower than the design value. This is because the actual mirror velocity is lower than the design value. Since speaker displacement versus applied voltage is calibrated under DC condition, when an AC signal is applied to the speaker, the speaker will exhibit a frequency response and its displacement will tend to be smaller than in DC. Therefore the real mirror velocity is smaller than the designed value and should be very close to the measured values in Fig. 6. If the frequency of AC bias is decreased, the difference be reduced.

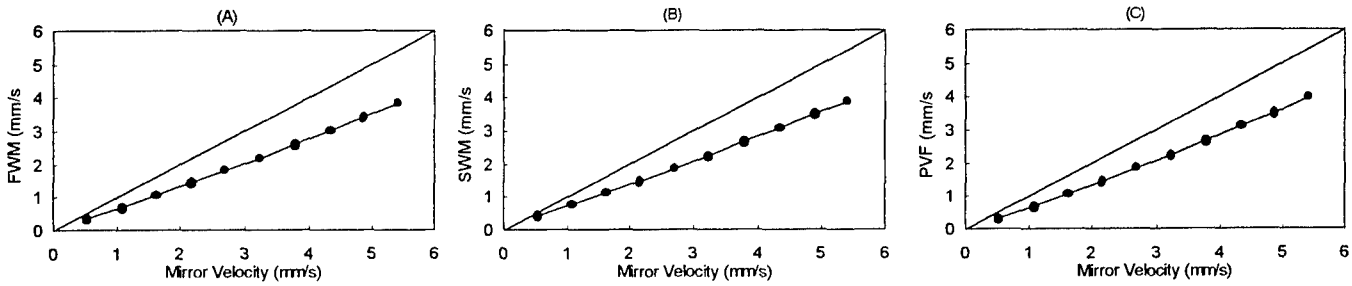

Fig. 6 Measured velocity versus mirror velocity for the (A) FWM (B) SWM algorithm and (C) PVF method

However, due to the indetermination of the conversion factor described in section 2, the important parameter is not the absolute value of an algorithm's output. It is the linearity with which algorithm responses to the simulator's velocity, that is, how straight the curves in Fig. 6 are. Table 1 shows the coefficient of determination $\mathbf{R^2}$ of the four sets of data. $\mathbf{R^2}$ is an indication of linearity of a set of data, with $\mathbf{R^2} = 1$ means perfectly linear and $\mathbf{R^2} = 0$ means totally unrelated. It can be observed from Table 1 that all three algorithms yield very good linearity with the mirror velocity.

Table 1 Coefficient of determination

Algorithm	Coefficient of Determination $\mathbf{R^2}$
First Weighted Moment	0.9991
Second Weighted Moment	0.9988
Peak Value Frequency	0.9991

5.2. In Vitro Experiment

The bandwidth is cut-off on 800Hz and line width is 1Hz in our experiment setup. Three groups of spectral response corresponding to different rotation rates are shown in Fig. 7. With an increase in fluid velocity, the fractions of the Fourier components are reduced at low frequencies and increase at high frequencies.

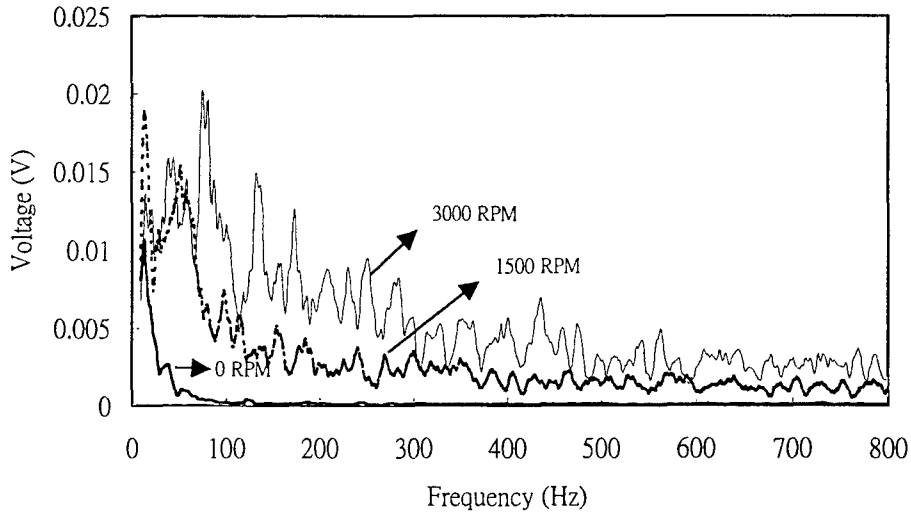

Fig. 7 Three groups of spectra corresponding to different velocities processed by moving average (10 periods)

Fig. 8 shows the computed velocities versus the DC motor's rotation rate. For each rotation rate, 20 samples were taken and averaged. According to the highly correlated relation between the rotation rates and the computed values employing FWM algorithm (R^2=0.9922), the derived value might be a reliable indicator to evaluate the relative fluid velocity. An indicator applying SWM is also provided. Though quite linear at high velocity measurement, it seemed to deviate at low velocity.

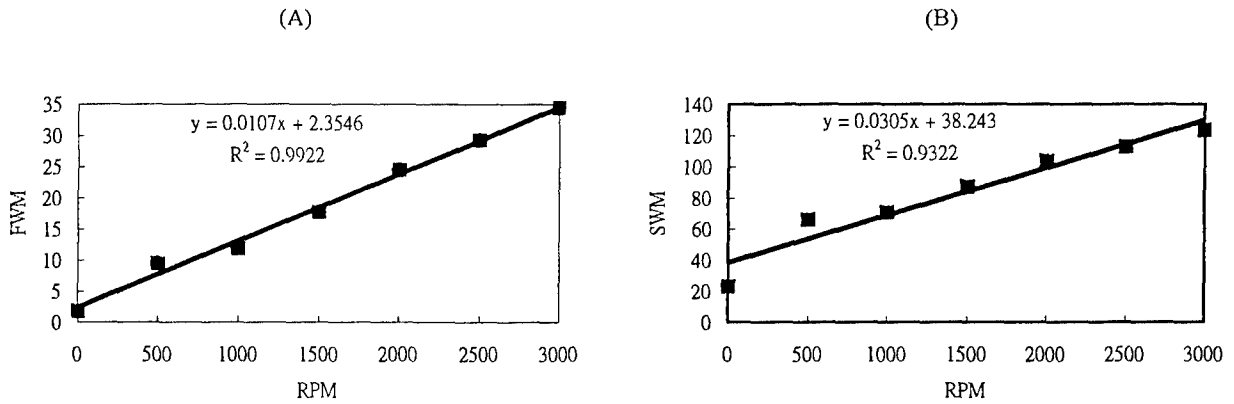

Fig. 8 (A) Relationship between FWM (in arbitrary unit), (B) SWM (in arbitrary unit) and Rotation Per Minute (RPM) of DC motor

6. CONCLUSIONS

We have developed a portable, real-time, and turn-key LDV system based on DSP techniques. Two most frequently used algorithms are adopted to test their linearity. Our outcome showed that both algorithms provide good indicators for fluid velocity measurement, and FWM seems to be a little better than SWM. Since different designs of simulation model and probe may also influence the corresponding results, more experiments should be taken to further evaluate the algorithms.

Now the in vivo experiment is taken on a cow. After installing a left ventricular assistant device on the cow, we use the LDV system to monitor its microvasculature. Information collected is used to evaluate the target's recovery, and helps the doctors to adjust the process of surgery.

ACKNOLWLEDGMENTS

The research is supported by the National Science Council (Taiwan) under grant contract no. NSC 89-2213-E-002 –055.

REFERENCES

1. T. W., D. J. Haumschild, D.W. Winsor, Y. Wang, and T. N. Luong, "Clinical application of laser Doppler flowmetry for measurement of cutaneous circulation in health and disease", The J. Vascu. Disea. **38**, pp. 727-736, 1987.
2. M.D. Stern, "In vivo evaluation of micro circulation by coherent light scattering", Nature **254**, pp. 56-58, 1975.
3. Martial H. Geiser, Ulrich Diermann, and Charles E. Riva, "Compact laser Doppler choroidal flowmeter", J.Biom. Opt. **4**, pp. 459-464, 1999.
4. G. Smedley, K. P. Yip, A. Wagner, S. Dubovitsky, and D. J. Marsh, "A laser Doppler instrument for in vivo measurements of blood flow in single renal arterioles", IEEE Trans. On Biomed. and Eng. **40**, pp. 290-297, 1993.
5. A. N. Obeid, N. J. Barnett, G. Dougherty, and G. Ward, "A critical review of laser Doppler flowmetry", J. Med. Eng. & Technol. **14**, pp. 178-181, 1990.

6. S. R. Arridge, M. Cope, and D. T. Delpy, "The theoretical basis for the determination of optical pathlengths in tissue: temporal and frequency analysis", Phy. Med. Biol. **37**, pp. 1531-1560, 1992.
7. L. Duteil, J. C. Bernengo, and W. Schalla, "A double wavelength laser Doppler system to investigate skin microcirculation", IEEE Trans. On Biomed. and Eng. **32**, pp. 439-445, 1985.
8. M. D. Stern, D. L. Lappe, P. D. Bowen, J. E. Chimosky, G.A. Holloway, JR., H.R. Keiser, and R. L. Bowman, "Continuous measurement of tissue blood flow by laser-Doppler spectroscopy", Am. J. Physiol. **232**(4), H441-H448, 1977.
9. A. N. Obeid, "In vitro comparison of different signal processing algorithms used in laser Doppler Flowmetry", Med.&Biol. Eng. & Comput. **31**, pp. 43-52, 1993.
10. A. N. Obeid, D. M. Boggett, N. J. Barnett, G. Dougherty, and P. Rolfe, "Depth discrimination in laser Doppler skin blood flow measurement using different lasers", Med. & Biol. Eng. & Comput. **26**, pp. 415-419, 1988.
11. M. H. Koelink, F. F. M. de Mul, J. Gereve, R. Graaff, A. C. M. Dassel, and J.G. Aarnoudse, "Laser Doppler blood flowmetry using two wavelengths: Monte Carlo simulations and measurements", Appl. Optics **33**, pp. 3549-3558, 1994.
12. M. J. C. Van Gerert, S. L. Jacques, H. J. C. M. Sterenborg, and W. M. Star, "Skin optics", IEEE Trans. On Biomed. Eng. **36**, pp. 1146-1154, 1989.
13. F. F. M. de Mul, M. H. Koelink, M. L. Kok, P. J. Harmsma, J. Gereve, R. Graaff, and J.G. Aarnoudse, " Laser Doppler velocimetry and Monte Carlo simulation on models for blood perfusion in tissue", Appl. Optics **34**, pp. 6595-6611, 1995.
14. R. Bonner, and R. Nossal, "Model for laser Doppler measurements of blood flow in tissue", Appl. Optics **20**, pp. 2077-2107, 1981.

*Correspondence : Email: gjjan@cc.ee.ntu.edu.tw; Telephone: (02)23635251-421(o)
Fax:(02)23671909; Taipei 10617, Taiwan